JOURNAL OF MOLECULAR SPECTROSCOPY 130, 269–287 (1988)

Rotational Analysis of the Red Electronic Emission System $A^3\Phi \rightarrow X^3\Delta$ of Diatomic Niobium Nitride (NbN)

J.-L. FEMENIAS,* C. ATHENOUR,† K. M. RAO, AND T. M. DUNN‡[1]

*Laboratoire d'Optique Atomique et Moleculaire, Universite de Nice, Parc Valrose, 06034 Nice Cedex, France; †G.R.O.U.P.E. 06, Universite de Nice, Parc Valrose, 06034 Nice Cedex, France; and ‡Department of Chemistry, University of Michigan, Ann Arbor, Michigan 48109

The (0,0) band of the red emission system of the diatomic molecule niobium nitride (NbN) has been rotationally analyzed and found to arise from an $A^3\Phi_r$–$X^3\Delta_r$ transition. Constants for the two states have been determined including the magnitude of the spin–orbit coupling constants in spite of their strong numerical correlation: The electronic states involved belong to case (a) coupling and no satellite bands are observed. That these results are consistent with those of similar molecules such as ZrO and TiO is verified. The asymmetry of the energy separations of the three subsystems $^3\Phi_4$–$^3\Delta_3$, $^3\Phi_3$–$^3\Delta_2$, and $^3\Phi_2$–$^3\Delta_1$ probably has its main origin in the perturbation of the $X^3\Delta_2(5\sigma 4d\delta)$ substate by the low-lying $^1\Delta$ state of the same electronic configuration. A significant line broadening for $J > 60$, particularly in the $^3\Phi_2$–$^3\Delta_1$ (0,0) subband, has been found. It is attributed to Λ doubling or hyperfine broadening due to spin uncoupling but has not been definitively analyzed at this time. No localized perturbations have been found in any of the subbands.

I. INTRODUCTION

The spectra of transition metal nitrides, oxides, and sulfides show a number of interesting features:

—*A large number of close-lying electronic states,* arising from unpaired metallic *d* electrons, and whose relative positions are impossible to calculate by ab initio methods.

—*The high multiplicities of these states,* which is a problem in itself, but also because these high multiplicities coexist with lower ones giving rise to two sets of disconnected electronic states; a major problem is to determine the relative positions of these two sets, in the absence of intercombination bands, since the relative positions cannot be theoretically calculated. Thus many electron configurations compete to yield the ground state: the $(5s\sigma^2 4d\delta)X^2\Delta$ assignment of Uhler in NbO (*1*) has been abandoned in favor of the $(5s\sigma 4d\delta^2)X^4\Sigma$ symmetry with hyperfine structure (*2*); the $X^4\Sigma$ hypothesis of Akerlind in ScO (*3*) has been replaced by the $(4s\sigma)X^2\Sigma(b_{\beta s})$ model (with hfs) (*4*, *5*). Both of these examples represent a change of hypothesis only about the lowest state. In the case of ZrO, where singlet–singlet and triplet–triplet transitions are simultaneously observed, there is also a problem of choice of the ground state between the lowest singlet, $(5s\sigma^2)^1\Sigma$, and the lowest triplet, $(5s\sigma 4d\delta)^3\Delta$, states. Recent studies (*6*) show that a relation may exist between singlet and triplet states which provides a preference for the singlet as the lower of the two.

[1] To whom all correspondence should be addressed.

0022-2852/88 $3.00

—*A nuclear hyperfine structure* which complicates the study of the odd Z-metal molecules, but which sometimes is definitive in the choice of symmetry for the states, as seen above for NbO and ScO. This extra feature can lead to very interesting information about the chemical bonding in the molecule (*2*).

Simple models that explain most of the experimental observations have been discussed: one of them, based on the simple concept of electron transfer from metal to oxygen, nitrogen, or sulfur, was reported by one of us (*5*). This model is only approximate but in some cases (see, for example, the pure precession effect between the $(4p\pi)A^2\Pi$ and the $(4p\sigma)B^2\Sigma$ states of ScO (*7*, *8*)) numerical results show a surprising degree of coincidence with it, thereby validating a highly localized approximation despite its oversimplification (*9*).

Niobium mononitride is distinguished because of the presence of many of the above features in its spectrum. It is also worth noting that solid NbN is an excellent superconductor at an Nb:N ratio of 1:1 (its critical temperature is 16 K) and the study of its "monomer" in the gas phase represents the first step of a possible cluster study which may lead to a better understanding of the electronic behavior of the species.

The first reported spectrum of NbN was that observed in 1969 by Dunn and Rao (*10*)[2] who described the $A^3\Phi$–$X^3\Delta$ system in the red region. Infrared absorption work in an argon matrix by Green *et al.* (*11*) did not bring any confirmation or invalidation of the ground state symmetry but LIF studies (*12*) support the assignment of the ground state as $X^3\Delta$. A numerical analysis of the red system, which is summarized in Section V of this paper, was made in 1975 (*13*, *14*) and pointed out the regular nature of both $X^3\Delta$ and $A^3\Phi$ states. No report on singlet states or systems has yet been published so that the problem of the relative energies of the $(5s\sigma 4d\delta)^3\Delta$ and the $(5s\sigma^2)^1\Sigma$ states still exists.

Hyperfine structure is a dominant feature of the NbN red system. This is not surprising because natural $^{93}_{41}$Nb has a nuclear spin of 9/2 with the largest magnetic moment of any known nucleus (6.1435 nuclear magnetons). The important hyperfine structure observed in the $A^3\Phi$–$X^3\Delta$ system of NbN has been studied by Femenias *et al.* (*15*). It confirms the large contribution of an *s* electron centered on the metal atom in the $X^3\Delta$ state; it also requires a significant hyperfine interaction in the $A^3\Phi$ state (which is one of the very few cases where it has been observed in an electronically excited state with grating resolution; see also HgH (*16*), CN (*17*), and BiO (*18*).

A recent publication by Pazyuk *et al.* (*19*) suggests a different analysis and presents both $A^3\Phi$ and $X^3\Delta$ states as inverted.

The aim of the present paper is multiple:

—First, we would like to show that the conclusions of Ref. (*19*) are not physically or numerically grounded (Section IV).

—Second, we would like to point out, in this special example, the possibility of determining separately highly correlated parameters such as spin–orbit constants in case (a)–case (a) transitions (Section V).

[2] T. M. Dunn has shown by isotopic substitution that the emitter of this observed spectrum is actually NbN and not NbO^+.

—Third, we present a complete set of molecular parameters which allow an independent description of both the $X^3\Delta$ and the $A^3\Phi$ states. These values represent more than an improvement over the earlier results of Ref. (*10*) since they lead to a satisfactory comparison with similar molecules and they give some ideas on the neighboring states of $A^3\Phi$ and, above all, of $X^3\Delta$ (Section VI).

II. EXPERIMENTAL DETAILS

Niobium nitride, NbN, was obtained in a flow system from the reaction of $NbCl_5$ vapor and active nitrogen (and also $^{15}N_2$) in a 2450-MHz microwave discharge (power $\sim$100 W) using helium as the supporting gas. The red system is easy to generate; it is very intense and only traces of nitrogen from residual air in a bad vacuum apparatus are sometimes sufficient to obtain it; this can be a problem in the study of the spectrum of NbO (*20*).

The spectra were photographed on Kodak 103aD, 103aF, and PanX plates and films, on a Jarrell–Ash 3.4-m Ebert spectrograph with a 300 lines/mm grating blazed in the first order at 57 000 Å.

In order to study the very different features of the (0,0) band of the red $A^3\Phi$–$X^3\Delta$ system (the very intense and crowded parts of the Q heads, as well as the weak resolved hyperfine components of low-J lines and the broadening of the weak high-J lines in the $^3\Phi_2$–$^3\Delta_1$ (0,0) subband), the system was photographed in the 9th, 10th, and 11th orders with slit widths ranging from 20 to 50 μm. Exposure times varied from 10 to 30 min but some weaker features required 60–90 min. In the red system, the resolution was about 500 000 and the reciprocal dispersion was approximately 4 Å cm^{-1}.

The wavelength calibration was a thorium discharge tube powered by the same generator as the NbN source. Because of the extent of the $A^3\Phi$–$X^3\Delta$ (0,0) band (16 000–16 900 cm^{-1}, i.e., 5900–6250 Å), it was not possible to photograph it on a single plate at high resolution so that independent calibrations were made for each subband; e.g., in the region of the $^3\Phi_4$–$^3\Delta_3$ and $^3\Phi_3$–$^3\Delta_2$ (0,0) subbands (5900–6100 Å), the thorium source gave more than 90 atomic lines of which around 70 were good for calibration. In each case these lines were fitted to a fourth-order polynomial with a standard deviation which did not exceed some thousandths of angstroms.

The wavelengths of the molecular lines were interpolated from this polynomial and converted to vacuum wavenumbers. Final errors in the molecular line positions are estimated as ± 0.01 cm^{-1}.

III. APPEARANCE OF THE EMISSION SPECTRUM: THE RED $A^3\Phi \rightarrow X^3\Delta$ SYSTEM

Under low resolution, the emission spectrum (Fig. 1) shows an intense vibrational sequence in the red. Less intense bands are observed in the yellow, the green, and the blue; the more intense of them are around 5740, 5840, and 5860 Å (*12*). All of the bands observed in the spectrum, so far, are degraded to lower frequencies.

As noted above, the red system is interpreted as the (0,0) sequence of the $A^3\Phi$–$^3\Delta$ transition. At high resolution (Fig. 2 and Ref. (*15*)), this part of the spectrum shows a number of features which confirm this hypothesis:

First, this system obviously looks like a triplet (case (a))–triplet (case (a)) transition except for an evident inequality of the subband separations, which is not surprising

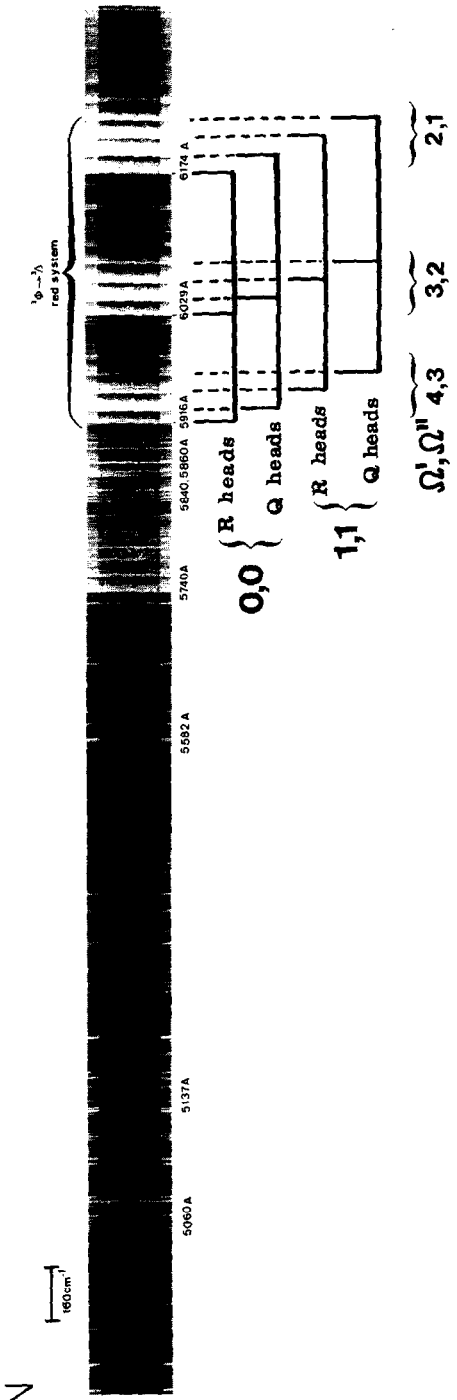

FIG. 1. The visible emission spectrum of NbN at low resolution.

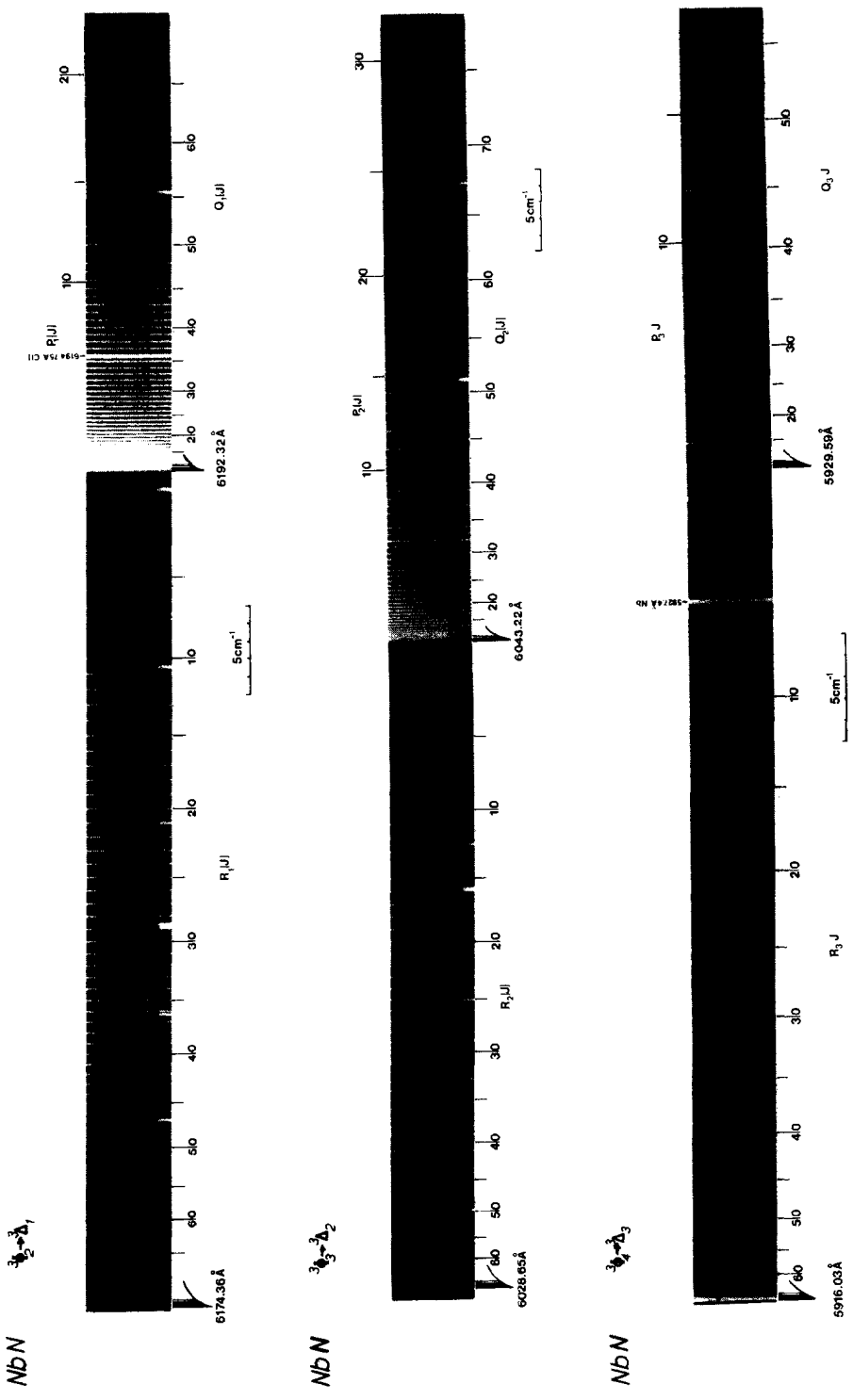

FIG. 2. The three (0,0) subbands of the red $A^3\Phi$–$X^3\Delta$ system of NbN at high resolution.

for such a molecule: one observes the same phenomenon in MoN (*21*) and NbO (*20*) and this indicates a strong perturbation of one of the states, or both of them.

Second, it was verified that *P*, *Q*, and *R* branches appear in each subband without any observable Λ doubling, which suggests that in the states involved, the internuclear axis component of the electronic orbital momentum, Λ, is greater than unity.

Finally, an important hyperfine splitting is observed (*10*, *15*) in both the $^3\Phi_4$–$^3\Delta_3$ (0,0) and the $^3\Phi_2$–$^3\Delta_1$ (0,0) extreme subbands which lie, respectively, around 5930 and 6190 Å; no hyperfine splitting is visible in the center $^3\Phi_3$–$^3\Delta_2$ (0,0) subband around 6040 Å. This hyperfine effect is observed only for low-*J* lines (*R* lines and some *Q* lines at grating resolution) and decreases rapidly with increasing *J* as expected for (a_β) coupling cases (*2*, *20*). The study of this hyperfine splitting (*15*) showed good agreement between the experimental observations (line position and intensity) and the theoretical calculations using a $^3\Phi(a_\beta)$–$^3\Delta(a_\beta)$ model. The dominant phenomenon is the magnetic Fermi contact effect in the ground $X^3\Delta$ state which confirms the $5s\sigma 4d\delta$ electron configuration of this state.

It is worth noting that a systematic broadening of the lines appears in the $^3\Phi_2$–$^3\Delta_1$ (0,0) subband as *J* increases and is clearly visible in all branches at $J \sim 70$ at grating resolution. This broadening is obvious in the *R* branch before the *R* bandhead, i.e., for $60 < J < 70$. Because of overlapping and decreasing intensity, it has been impossible to study this effect quantitatively at this time. The broadening seems to be accompanied by a significant decrease in intensity (Fig. 3a). In the *P* branch (Fig. 3b) the structure is less crowded than in the *R* branch and, despite overlapping of the $A^3\Phi_2$–$X^3\Delta_1$ (1,1) subband, *P* lines of the (0,0) band are clearly observed up to $J \cong 70$; the broadening is obvious for $J \cong 60$. When *J* increases to 70, the linewidth increases up to three times the "standard" rotational linewidth, i.e., three times the width of a line at $J \sim 30$ where the hyperfine splitting is insignificant. The overlapping $A^3\Phi_2$–$X^3\Delta_1$ (2,2) subband hinders any further observation for $J > 70$. In the *Q* branch (Fig. 3c) observation can be made up to $J \sim 80$ and the *Q* linewidth increases to more than three times the "standard" linewidth at this stage.

No localized perturbation was observed in the $A^3\Phi$–$X^3\Delta$ (0,0) band of NbN. This is important for the validity of the numerical approach used below (Section V).

IV. CLASSICAL ANALYSIS AND DISCUSSION ON REGULARITY OF THE STATES

The frequencies of the lines in the $A^3\Phi$–$X^3\Delta$ (0,0) band of NbN are given in Table I. The low-*J* *P* and *Q* lines are very difficult to pick out in the crowded regions of the subbandheads; the determination of their wavenumbers necessitates a sub-Doppler study, especially in the $^3\Phi_2$–$^3\Delta_1$ and $^3\Phi_4$–$^3\Delta_3$ subbands where these regions are complicated by the large hyperfine splitting. Despite the high quality of the spectrum, in the regions of low-*J* *R* lines, the line wavenumbers cannot be given for the lowest *J* values because of hyperfine splitting, except in the $^3\Phi_3$–$^3\Delta_2$ (0,0) subband where this splitting is not observed and where the wavenumbers of the *R* lines are precisely measurable from the lowest ($J = 2$) value.

A first rough analysis can be made considering each $^3\Phi_{\Omega'}$–$^3\Delta_{\Omega''}$ subband as an independent singlet–singlet transition. The absence of observable Λ doubling in these

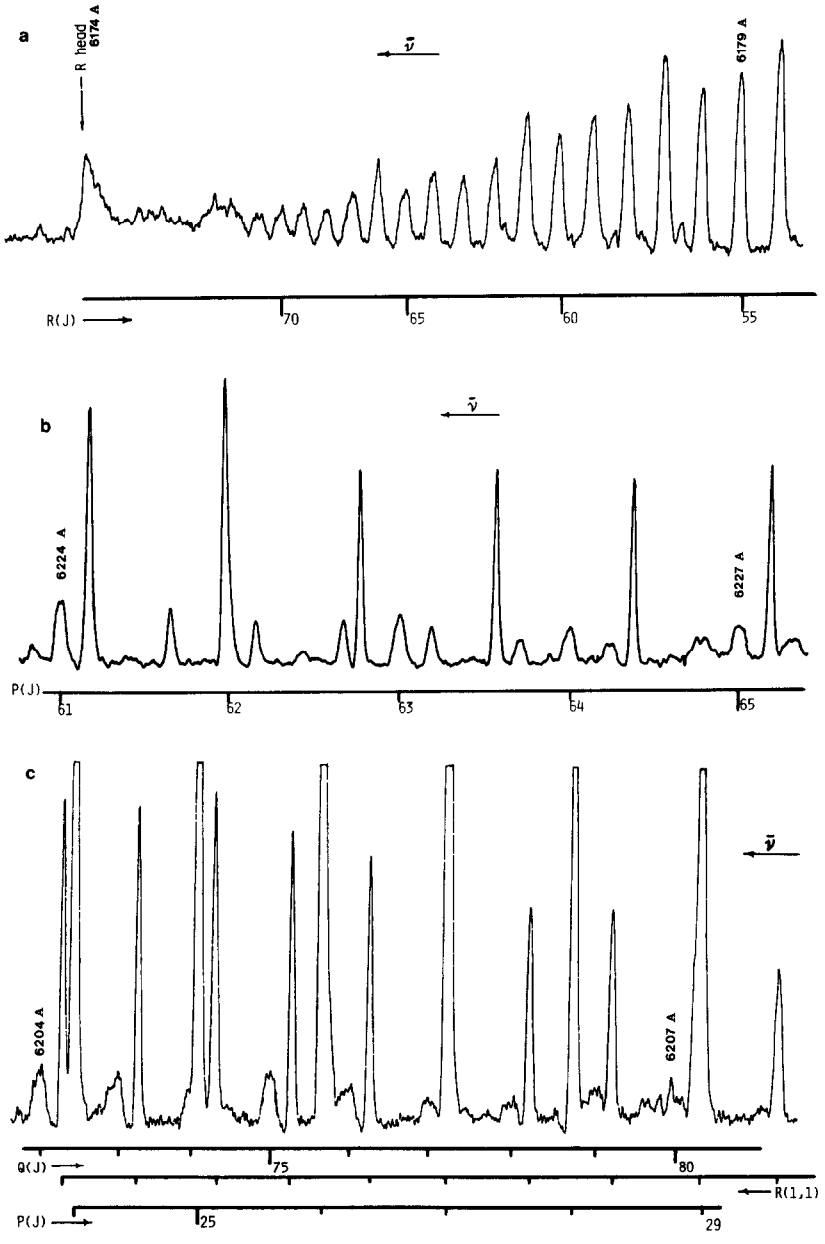

FIG. 3. Line broadening in the $A^3\Phi_2$–$X^3\Delta_1$ (0,0) subband of NbN. (a) R branch; (b) P branch; (c) Q branch

transitions leads to a very simple theoretical model for the rotational levels, taking into account only the centrifugal stretching and using effective parameters:

$$F(J) = T_0 + B_{\text{eff}}J(J+1) - D_{\text{eff}}J(J+1)^2. \quad (1)$$

In order to use all the information given in Table I, especially in the Q branches whose lines can be measured to higher J than the P or R branches, the combination

TABLE I

Wavenumbers of the Rotational Lines in the (0,0) Band of the Red $A^3\Phi$–$X^3\Delta$ System of NbN

	$^3\Phi_2$ — $^3\Delta_1$			$^3\Phi_3$ — $^3\Delta_2$			$^3\Phi_4$ — $^3\Delta_3$		
J	P	Q	R	P	Q	R	P	Q	R
1			hfs						
2		bh/hfs	hfs			16545.932			
3	bh/hfs	bh/hfs	hfs		bh	546.883			A/hfs
4	bh/hfs	bh/hfs	hfs	bh	bh	547.822		bh/hfs	hfs
5	bh/hfs	bh/hfs	hfs	bh	bh	548.757	bh/hfs	bh/hfs	A/hfs
6	bh/hfs	bh/hfs	hfs	bh	bh	549.670	bh/hfs	bh/hfs	hfs
7	bh/hfs	bh/hfs	hfs	bh	16542.643	550.583	bh/hfs	bh/hfs	hfs
8	bh/hfs	bh/hfs	hfs	16534.615	542.552	551.473	bh/hfs	bh/hfs	hfs
9	bh/hfs	bh/hfs	hfs	533.529	542.448	552.363	bh/hfs	bh/hfs	hfs
10	bh/hfs	bh/hfs	16155.013	532.423	542.330	553.232	bh/hfs	bh/hfs	16870.550
11	bh/hfs	bh/hfs	155.901	531.288	542.194	554.098	16848.682	bh/hfs	871.408
12	bh/hfs	bh/hfs	156.772	530.182	542.055	554.942	847.508	16859.421	872.246
13	16130.891	16143.762	157.632	529.017	541.905	555.780	846.446	859.271	873.076
14	129.784	143.626	158.486	527.863	541.741	556.599	845.203	859.008	873.894
15	128.650	143.484	159.331	526.710	541.563	557.419	843.883	858.830	874.694
16	127.494	143.330	160.164	525.536	541.368	558.211	842.763	858.627	875.484
17	126.321	143.170	160.996	524.316	541.168	559.006	841.555	858.409	876.272
18	125.174	142.997	161.797	523.131	540.956	559.779	840.333	858.189	877.037
19	123.937	142.814	162.607	521.898	540.731	560.544	839.126	857.951	877.800
20	122.817	142.620	163.399	520.683	540.488	561.298	837.799	857.701	878.531
21	121.625	142.410	164.188	519.453	540.242	562.030	836.609	857.444	879.261
22	120.425	142.196	164.958	518.194	539.985	562.765	835.312	857.170	879.984
23	119.214	141.972	165.718	516.934	539.712	563.474	834.070	856.881	880.681
24	117.990	141.741	166.473	515.655	539.434	564.175	832.782	856.578	881.371
25	116.765	141.498	167.221	514.372	539.122	564.875	831.423	856.267	882.042
26	115.523	141.246	167.945	513.078	538.815	565.541	830.163	855.943	882.706
27	114.265	140.981	168.680	511.762	538.494	566.216	828.830	855.603	883.360
28	113.007	140.703	169.337	510.462	538.163	566.864	827.494	855.250	883.995
29	111.754	140.420	170.088	509.115	537.820	567.499	826.143	854.389	884.626
30	110.462	140.129	170.787	507.773	537.460	568.139	824.778	854.516	885.234
31	109.180	139.824	171.462	506.422	537.090	568.748	823.409	854.127	885.832
32	107.879	139.513	172.138	505.049	536.707	569.353	822.013	853.729	886.416
33	106.573	139.181	172.788	503.666	536.316	569.944	820.616	853.313	886.990
34	105.253	138.849	173.446	502.280	535.912	570.523	819.201	852.885	887.551
35	103.932	138.500	174.082	500.875	535.484	571.089	817.778	852.445	888.097
36	102.589	138.145	174.711	499.455	535.055	571.646	816.337	851.991	888.631
37	101.245	137.796	175.331	498.029	534.615	572.187	814.884	851.526	889.151
38	099.838	137.419	175.932	496.590	534.169	572.709	813.423	851.052	889.658
39	098.516	137.032	176.529	495.146	533.697	573.223	811.948	850.558	890.139
40	097.135	136.640	177.117	493.683	533.211	573.730	810.461	850.053	890.622
41	095.732	136.236	177.692	492.183	532.727	574.217	808.956	849.537	891.092
42	094.365	135.822	178.262	490.726	532.223	574.686	807.436	849.002	891.538
43	092.931	135.385	178.814	489.227	531.699	575.156	805.908	848.461	891.974
44	091.547	134.958	179.350	487.715	531.170	575.604	804.362	847.903	892.402
45	090.146	134.516	179.890	486.225	530.632	576.039	802.850	847.328	892.312
46	088.691	134.044	180.404	484.658	530.071	576.462	801.254	846.759	893.203
47	087.251	133.586	180.914	483.089	529.503	576.874	799.679	846.156	893.578
48	085.804	133.111	181.413	481.533	528.932	577.276	798.088	845.546	893.961
49	084.319	132.612	181.895	479.983	528.337	577.656	796.486	844.923	894.314
50	082.844	132.109	182.376	478.401	527.733	578.023	794.894	844.285	894.652
51	081.344	131.612	182.839	476.815	527.115	578.386	793.240	843.641	894.986
52	079.851	131.085	183.298	475.193	526.481	578.737	791.613	842.961	895.305
53	078.339	130.554	183.741	473.573	525.845	579.068	789.909	842.299	895.601
54	076.836	130.012	184.160	471.955	525.187	579.382	788.279	841.602	895.884
55	075.310	129.457	184.580	470.311	524.514	579.682	786.618	840.901	896.153
56	073.788	128.891	184.987	468.645	523.838	579.916	784.900	840.185	896.404
57	072.232	128.323	185.383	466.981	523.131	580.249		839.450	896.655
58	070.640	127.727	185.759	465.311	522.418	580.514		838.704	896.881
59	069.103	127.139	186.137	463.621	521.716	580.770		837.947	897.103
60	067.551	126.528	186.503	461.911	520.973	581.003		837.179	897.296
61	065.936	125.903	186.844	460.176	520.247	581.218		836.382	897.473
62	064.367	125.290	187.185	458.471	519.453	581.430		835.597	897.645
63	062.728	124.633	187.507	456.718	518.700	581.618		834.768	897.802
64	061.108	123.987	187.825	454.965	517.928	581.805		833.956	897.948
65	059.476	123.322	188.120	453.197	517.111	581.966		833.079	
66	057.862	122.645	188.410	451.422	516.298	582.127		832.261	
67	056.172	121.964	188.681	449.583	515.448	582.266		831.423	
68	054.521	121.257	188.951	447.825	514.636	582.391		830.507	
69	052.840	120.547	189.204	446.006	513.777	582.493		829.609	
70		119.818	189.432	444.165	512.918			828.649	
71		119.094	189.666		511.992			827.768	
72		118.344			511.140			826.823	
73		117.577			510.224			825.861	
74		116.765			509.306			824.907	
75		116.043			508.371			823.909	
76		115.247			507.418			822.916	
77		114.417			506.422			821.907	
78		113.623			505.486			820.878	
79		112.798			504.497			819.838	
80					503.484			818.773	
81					502.421			817.778	
82					501.429			816.623	
83					500.389				
84					499.350				
85					498.251				
86					497.163				
87					496.038				
88					494.933				

Note. Experimental uncertainties are estimated as 0.01 cm^{-1}. A, bh: line blended with an atomic line or n a bandhead region; hfs: no value because of large hyperfine splitting. All units are reciprocal centimeters.

TABLE II

Effective Rotational Parameters in the $A^3\Phi$–$X^3\Delta$ (0,0) Band of NbN

	$^3\Delta$ state			$^3\Phi$ state		
	$^3\Delta_1$	$^3\Delta_2$	$^3\Delta_3$	$^3\Phi_2$	$^3\Phi_3$	$^3\Phi_4$
B_{eff}	0.50015(5)	0.50160(5)	0.50263(6)	0.49532(5)	0.49570(5)	0.49642(6)
$10^6 D_{eff}$	0.471(7)	0.459(7)	0.454(11)	0.495(7)	0.488(7)	0.484(11)
Origins	← $T_2'-T_1'' = \bar{\nu}_{21}$ = 16144.648(3) →					
of the		← $T_3'-T_2'' = \bar{\nu}_{32}$ = 16542.980(3) →				
sub-bands			← $T_4'-T_3'' = \bar{\nu}_{43}$ = 16860.319(4) →			

The number in parentheses is the uncertainty in the last digit that corresponds to two standard deviations. The r.m.s. obtained with these parameters is 0.009. All units are reciprocal centimeters.

relation method was not used and, despite the simplicity of the theoretical model, the experimental data were reduced using the well-known direct approach (*14*, *22*).

It is impossible to determine the vibronic energies (T_0) of all substates; one can only obtain the differences $\nu_{\Omega'\Omega''} = T_{0\Omega'} - T_{0\Omega''}$ between these origins, where the subscripts Ω' and Ω'' represent, respectively, the upper and lower Ω value in the transition.

The results are summarized in Table II. The standard deviation obtained when recalculating the lines with these parameters is 0.009 cm^{-1}, which corresponds to the estimated uncertainty. This may be considered a test of good fit.

At this point, we need to point out some important details:

First, we remark that the preceding classical procedure is simple and efficient. Thus, it is not spoiled by any problem of the Hamiltonian model and it is independent of the assignment of any other band. The standard deviation obtained is a proof of the validity of the choice of the term energies; the accuracy of the results (see Table II) can be compared with advantage with Ref. (*19*). The trace invariance of the $^3\Phi$ and $^3\Delta$ rotational Hamiltonian operator under a similarity transformation gives the real B and D values of both states as simple averages of the B_{eff} and D_{eff} values of the spin components (*23*, *24*). The results of this calculation are given in Table III and show a very large difference with the values of Ref. (*19*).

Second, as shown by hyperfine studies (*15*), the contribution of an s electron in the $X^3\Delta$ ground state is obvious and important; this leads, of course, to a good $(s\sigma)\delta$ approximation of the ground state wavefunction (which is identified, as seen above, with essentially $5s\sigma 4d\delta$). This determinantal approximation yields the regularity of the $X^3\Delta$ ground state because, in such a case, the spin–orbit parameter A_Δ is identical to the positive quantity $a_\delta/2$, where a_δ is the monoelectronic spin–orbit parameter in the Hamiltonian form $H_{SO} = \sum_i a_i \mathbf{l}_i \mathbf{s}_i$, and is analogous to the positive atomic ξ parameter (*25*). The differences $\bar{\nu}_{\Omega'\Omega''}$ given in Table II show that the regularity of the $X^3\Delta$ state yields that of the excited $A^3\Phi$ state. However, a similar reasoning can be made for the $A^3\Phi(\pi\delta)$ state, which leads to the positive value $(a_\pi/6 + a_\delta/3)$ for A_Φ. We shall use below this expression for A_Φ, but one must keep in mind that the deter-

TABLE III

Rotational B Parameters and Centrifugal Stretchings D of the $A^3\Phi$ ($v = 0$) and $X^3\Delta$ ($v = 0$) Levels of NbN from the Results of Table II (See Text)

	$X^3\Delta$ state	$A^3\Phi$ state
B*	0.50146(5)	0.49581(5)
10^6 D	0.462(8)	0.489(8)
A*	~200	~300

Note. Evaluation of the spin–orbit parameters A_Φ and A_Δ of the same levels of NbN from Table IV. This set of parameters is used as a starting set for the nonlinear (direct approach) fit leading to the results given in Table VII. All units are reciprocal centimeters.

minantal approximation of $A^3\Phi$ is not as simple as that of $X^3\Delta$ because of the expected mixing, *inter alia,* of $4d\delta 4d\pi$ and $4d\delta 5p\pi$ and other possible configurations.

Thus the discrepancy between the present results and those of Ref. (*19*) for the B and D parameters of both states could have its origin in the fact that $X^3\Delta$ and $A^3\Phi$ are not inverted. An alternative assignment of the supposed "satellite bands" (*19*) has been proposed (*12*) but is beyond the scope of the present paper; this will be published later. In fact, after these qualitative suggestions, we now need more quantitative proposals: two possibilities are offered, and they are our third and fourth points.

Third, a very simple and usual way to roughly predict the magnitude of spectroscopic constants is the comparison with other ("similar") molecules. In our case, the concept of "similarity" is very wide because we only need molecules in which the two open shells are essentially metallic and of the same symmetry as those of consideration in NbN, i.e., $(n + 1)\,s\sigma nd\delta$ for $^3\Delta$ and $nd\delta nd\pi$ or $nd\delta(n + 1)p\pi$ for $^3\Phi$. Simple scaling using a convenient ratio of atomic metal $\xi(d)$ values (*26*) can give a reasonable evaluation of A_Δ(NbN) from the value of the same parameter in the corresponding "similar" molecule. The same procedure can be attempted for A_Φ, assuming in this case a pure $nd\delta nd\pi$ configuration in both molecules. Evaluations of A_Δ and A_Φ for NbN from ZrO and TiO data (*27*) are given in Table IV.

Fourth and finally, there exists a different "internal" way to assess if an electronic state is regular or not and to estimate the value of its spin–orbit parameter. It follows from the formula first derived by Mulliken (*28*) and which can also easily be derived from Eq. (6), p. 69, of Ref. (*23*), for triplets,

$$|A| = \frac{4B^2}{\Lambda\{B_{\text{eff}}(\max) - B_{\text{eff}}(\min)\}}, \tag{2}$$

where $B_{\text{eff}}(\max)$ is the larger value of B_{eff} among the three substates, which is always associated with the upper substate, and $B_{\text{eff}}(\min)$ is the lower one associated with the lower substate. If, as in our case, the larger (resp. lower) B_{eff} is assigned to the $\Omega = \Lambda$

TABLE IV

Evaluation of the Spin–Orbit Parameters A_Δ and A_Φ of the $X^3\Delta$ ($v = 0$) and $A^3\Phi$ ($v = 0$) Levels of NbN from Data of Similar Molecules, following the Two Procedures Described in the Text

		ZrO	TiO	TiS	NbN	YF[a]	ScF	NbN
A_Δ	as $\frac{^3\Delta_3 \to {}^3\Delta_1}{4}$	156.4	49.4	46.3				least squares fit of the $A^3\Phi \to X^3\Delta(0,0)$ band of NbN (Table VII)
	from B_{eff}	140.3		50.1	202.8	82.7	32.4	
A_Φ	as $\frac{^3\Phi_4 \to {}^3\Phi_2}{6}$	205.4	56.9					
	from B_{eff}	165.9			298.0	164.0	41.6	
Scaling to NbN								
	A_Δ	211.6	211.6	198.2	202.8	166.6	219.7	182.99
	A_Φ	278.0	243.6		298.0	330.3	282.9	241.60

Note. When the value of the spin–orbit parameter is available together with the B_{eff} values, Eq. (3) is used in order to check its validity (ZrO: $X^3\Delta$ and $A^3\Phi$; TiS: $X^3\Delta$).

[a] Data are from Ref. (*27*), except for YF (*29*). All units are reciprocal centimeters.

$+ S$ (resp. $\Omega = \Lambda - S$) substate, then the electronic state under consideration is regular. This remark yields the algebraic form for triplets:

$$A = \frac{4B^2}{\Lambda\{B_{eff}(\Sigma = +1) - B_{eff}(\Sigma = -1)\}}. \tag{3}$$

This formula is valid when the electronic state is near an (a) coupling case with a possible slight (b) tendency (spin uncoupling). Case (c) tendencies must be very weak if one requires a reasonable quantitative evaluation of A.

Of course such a formula may also be applied to "similar" molecules where only B_{eff} values are available, in order to obtain their spin–orbit parameter A; the same scaling procedure by $\xi(d)$ values as above has been used to obtain the evaluation of the A parameters in NbN. The estimates of A_Δ and A_Φ for NbN from NbN itself, YF, and ScF are given in Table IV.[3]

Rough evaluations of the spin–orbit parameters of NbN are thus easily available ($A_\Delta \sim 200$ cm^{-1} and $A_\Phi \sim 300$ cm^{-1}) which confirm once again and quantitatively the regular nature of $X^3\Delta$ and $A^3\Phi$.

It is now necessary to endeavor to obtain more accurate values of these parameters.

V. DETERMINATION OF THE SPIN COMPONENT SEPARATIONS

(a) Some Introductory Remarks

The knowledge of the spin component separations in an electronic multiplet is of great physical and chemical interest. In a case (a)–case (a) transition, the absence of

[3] As a test, this formula was used in the case of the $\sigma\delta^3\Delta$ and $\pi\delta^3\Phi$ states of ZrO and the $\sigma\delta^3\Delta$ state of TiS where the values of A_Δ and A_Φ are available. The results of the calculation are also given in Table IV.

TABLE V

Rotational Hamiltonian Operator for a Triplet State with $\Lambda > 1$

	$\lvert\Lambda,\Sigma=1\rangle$	$\lvert\Lambda,\Sigma=0\rangle$	$\lvert\Lambda,\Sigma=-1\rangle$
$\langle\Lambda,\Sigma=1\rvert$	$T_o^* + A^*\Lambda + (B^* + 2A_J\Lambda)(X - 2\Lambda)$ $-D[(X-2\Lambda)^2 + 2(X-\Lambda)]$	$-[2(X-\Lambda)]^{1/2}[B^* + A_J\Lambda + p]$ $-2D(X-\Lambda+1))$	$-2D(X^2-\Lambda^2)^{1/2}$
$\langle\Lambda,\Sigma=0\rvert$	symm.	$T_o^* + \delta + B^*(X+2)$ $-D[(X+2)^2 + 4X]$	$-[2(X+\Lambda)]^{1/2}[B^* - A_J\Lambda + p$ $-2D(X+\Lambda+1)]$
$\langle\Lambda,\Sigma=-1\rvert$	symm.	symm.	$T_o^* - A^*\Lambda + (B^* - 2A_J\Lambda)(X+2\Lambda)$ $-D[(X+2\Lambda)^2 + 2(X+\Lambda)]$

The condition $\Lambda > 1$ indicates that we do not take into account the fourth-order Λ-doubling terms. $X = J(J+1) - \Lambda^2$.

satellite bands makes their determination difficult. However, in practice, no case (a) coupling is pure and spin-uncoupling effects produce deviations from the pure case (a) expressions of the energy which increase with J and which depend on the ratio B/A. These deviations are the origin of the formula (3); numerically, their characteristic behavior as a function of J sometimes may allow a determination of A.

One may argue that parameters such as A are highly correlated in a case (a)–case (a) transition. But, first, B' and B'' are also highly correlated (*30*) and are the most precisely determined molecular parameters, which shows that correlation is not the unique criterion for parameter determination. Second, in spite of appearance, the exact significance of correlation is not clearly established (*31*); this latter discussion is beyond the scope of this paper and will be published later.

Our method is a simple direct approach procedure (*14*, *22*), using rotational Hamiltonian operators for triplet states ($\Lambda > 1$) as given in Table V (*24*, *32*). The slight differences between our matrix and that of Veseth (*24*) lie in the choice and the definition of the independent parameters; the correspondence is given in Table VI and our notations are visualized in the $^3\Phi$(case (a))–$^3\Delta$(case (a)) transition diagram of Fig. 4.[4]

The starting parameters are those given in Table III and the results of this least-squares fit are summarized in Table VII.

(b) The Numerical Procedure

Before analyzing these results, we want to dwell upon the fact that many precautions were taken in order to check their numerical validity. More details about this study

[4] In the following, the parameter δ will be referred to as the "central shift" parameter.

TABLE VI

Notation of This Work Compared to That of Ref. (*24*)

This work	T_o^*	A^*	A_J	δ	B_{eff}	D	p
Veseth (24)	$T_{eff}+\varepsilon-\gamma+\frac{\alpha'_{-1}+\alpha'_1}{2}$	$A+\frac{\alpha'_1-\alpha'_{-1}}{2}$	A_J	$-3\varepsilon-\gamma+\alpha_o-\frac{\alpha'_{-1}+\alpha'_1}{2}$	B_{eff}	D	$\frac{1}{2}\gamma_{eff}$

are given in Ref. (*14*); we only summarize it here. A number of synthetic $^3\Phi$–$^3\Delta$ transitions were studied following the technique of Albritton *et al.* (*30*), all of them being calculated with parameters of the same order of magnitude as those of NbN (see Tables III and VII). Three main empirical conclusions are to be noted:

(i) If A_J and p (see Table V) are not introduced in the original set of parameters, the other parameters are correctly reproduced by the least-squares fit. Of course the spin–orbit parameters are determined increasingly badly when one increases the artificial Gaussian uncertainty of the synthetic spectrum: the uncertainty hides the spin-uncoupling effects in B/A which allow the separate determination of the A's. With an uncertainty of the order of magnitude of our experimental one, the spin–orbit A's are fairly reproduced.

(ii) Very drastic problems arise when A_J and/or p are introduced in the original set of parameters, and in such cases, partial "by hand" grid searches are necessary to force the convergence. However, it turns out clearly that in such cases a correct fit is impossible without A_J and/or p. The logical contraposition of this sentence is the following: "if a correct fit can be obtained without A_J and/or p, then A_J and/or p are negligible." At first glance this statement appears to be a truism. A simple example may convince

TABLE VII

Parameters of the $A^3\Phi$ ($v = 0$) and $X^3\Delta$ ($v = 0$) Levels of NbN from the Nonlinear (Direct Approach) Fit

	$X^3\Delta$ state	$A^3\Phi$ state
T_0^*	fixed at 0	16504.938(1)
A^*	183.01(7)	241.61(5)
δ	-33.09(8)	7.42(8)
B^*	0.50145(2)	0.49580(2)
10^6D	0.462(3)	0.493(3)
10^5A_J	-2.20(22)	-1.44(14)
p	insignificant	insignificant

Note. All units are reciprocal centimeters. The numbers in parentheses correspond to one standard deviation on the last digit. The rms obtained with these parameters is 0.011. Tests with A_J and p fixed at zero lead to an rms of 0.012. The uncertainty in each parameter is less than 15 times the corresponding standard deviation in order to obtain a confidence probability of 95%.

the reader that this is not the case: consider the $A^2\Pi$ state with a large centrifugal stretching on A (A_J) and a negligible spin–rotation effect (γ); a numerical study of this state with a Hamiltonian model including γ but not A_J will lead to a satisfactory fit and to the physical conclusion that the spin–rotation effect is important, which is not correct. The correlation between γ and A_J enables one effect to be entirely absorbed by the other one. In our present case it is clear that the effects of A_J or p in the states of interest are numerically original and that if A_J and/or p are not *numerically* necessary then they are *physically* negligible.

(iii) Finally let us point out the fact that our synthetic data are ideal in the sense that only a Gaussian uncertainty affects them. No systematic errors were introduced nor, above all, were perturbations. A trial calculation was made with the experimental data of the $C^3\Delta$–$X^3\Delta$ (0,0) transition of TiS (*33*)[5] where the upper spin components $C^3\Delta_1$ and $C^3\Delta_2$ are slightly perturbed. We verified that the calculated spin–orbit constants ranged from no less than 400 to 50 cm^{-1} (instead of the real values $\sim$46 cm^{-1}) in the successive tests made by progressively eliminating the perturbed data. In such a case, a classical technique (*33*) is necessary in order to correctly guide the numerical approach.

(c) Results from the NbN Experimental Data (Table VII)

A very good standard deviation (0.012 cm^{-1}) is obtained without A_J or p in both states. With the introduction of the A_J's the standard deviation improves slightly (0.011 cm^{-1}) but p parameters have no effect: thus we obtain the order of magnitude of both A_J's and we conclude that p parameters are negligible in both states.

Compared to the standard deviation obtained with the very flexible "effective" analytic model (Eq. (1): 0.009 cm^{-1}) such standard deviations appear as very good results. The slight differences with the preceding standard deviation is clearly attributable to the rigidity of the more rigorous matrix model (Table V).

The spin–orbit parameters A_Φ and A_Δ are less important than expected (see Table III) but the orders of magnitude are good. They are "fairly" determined when one considers the circumstances of such a calculation (case (a)–case (a) transition and correlation coefficient of A_Φ and A_Δ very close to 1, more precisely, 0.99999). In fact several details need to be pointed out: there are 571 rotational lines from $J = 1$ to $J = 88$ with a good grating accuracy and without evidence of any perturbation or systematic deviation; the values of A_Φ and A_Δ are large, together with values of B/A which lead to noticeable spin-uncoupling deviations. With the fact that the correlation coefficient between A_Φ and A_Δ is not *strictly* 1, these details enable one to understand the statistical explanation of such an apparently surprising determination (*31*). The relative positions of the spin components in the $A^3\Phi$ ($v = 0$)–$X^3\Delta$ ($v = 0$) transition of NbN are represented in Fig. 4. As can be seen, the central shifts δ are not very important (for comparison see the cases of NbO (*20*) and MoN (*21*)), but are opposite in each state thereby leading to a more drastic effect in the spectrum.

The values of the B and D parameters are very close to those expected (Table III) and the reader can verify that this agreement exists even with uncertainties equal to

[5] The authors thank Professor R. F. Barrow for kindly sending them the experimental data concerning this molecule.

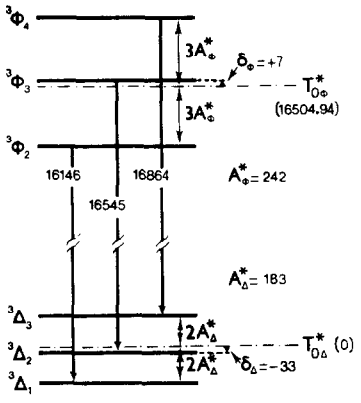

FIG. 4. Energy level diagram for the $A^3\Phi$(case (a))–$X^3\Delta$(case (a)) transition of NbN. The numerical data are those of Table VII. All units are reciprocal centimeters.

one standard deviation. However, the evidence of systematic deviations in the residuals of this last direct approach—but not in the preceding "effective" one—points out that there is a lack of normality in the statistical distributions. This effect probably arises from what we called the "rigidity" of the matrix model of Table V. More precisely, this classical model fails somewhat in reproducing the interactions with other electronic states. This issue will be dealt with, and partially corrected, in the next section.

The main effect of this lack of normality lies in the evaluation of the confidence intervals for the parameters. The usual 3 standard deviations should be replaced by 15 standard deviations when the number of parameters is ~ 10 (here we have 9 to 13) with a confidence probability of 95% (*31*). The uncertainty in the spin–orbit parameters is thus ~ 1 cm^{-1}, a remarkably small value when one considers their correlation. The uncertainty in the rotational parameters is 0.0003 cm^{-1} which is a relatively large one. This can physically be explained by the large influence which the $^1\Delta$ state has on the $X^3\Delta$ state (and probably the effect of $^1\Phi$ on $A^3\Phi$—see next section): this source of case (c) tendency is not taken into account by our Hamiltonian matrix model (Table V) so that the fit is partially inadequate and leads to a bias on all of the parameters. On the other hand, comparison of the values of the "effective" and the "matrix" approach shows that the need of a more sophisticated matrix model is not imperative at this time.

VI. DISCUSSION

In this section, we would like to initiate some explanation of the asymmetries found in both $X^3\Delta$ and $A^3\Phi$ states of NbN. Note that such asymmetries were also found in the similar states of ZrO and TiO (*27*).

Such effects are caused by a second-order spin–orbit interaction with neighboring states: they are $\Delta\Omega = 0$ perturbations which give rise to case (c) tendencies (very slight ones in the present case). With the addition of the $\Delta\Lambda = 0, \pm 1$ rule, a number of possible perturbing states can be found for each of the $X^3\Delta$ and $A^3\Phi$ states. However,

this number can be reduced if one takes advantage of the most probable electron configurations of these states.

1. The Ground $X^3\Delta(5s\sigma 4d\delta)$ State

For brevity, the ground $X^3\Delta(5s\sigma 4d\delta)$ state can be represented by the following determinantals:

$$
\begin{aligned}
{}^3\Delta_3 &= \sigma\delta \\
{}^3\Delta_2 &= \frac{1}{\sqrt{2}}(\bar{\sigma}\delta + \sigma\bar{\delta}) \\
{}^3\Delta_1 &= \bar{\sigma}\bar{\delta}.
\end{aligned} \tag{4}
$$

The last member of this set is given by the orthogonal ${}^1\Delta_2$ state

$$
{}^1\Delta_2 = \frac{1}{\sqrt{2}}(\bar{\sigma}\delta - \sigma\bar{\delta}). \tag{5}
$$

It is readily verified that the effect of the simple phenomenological monoelectronic spin–orbit operator

$$
H_{SO} = \sum_i a_i \mathbf{l}_i \mathbf{s}_i \tag{6}
$$

on the ${}^3\Delta_\Omega$ wavefunctions results in

$$
\begin{aligned}
H_{SO}{}^3\Delta_3 &= a_\delta \sigma\delta &&= a_\delta {}^3\Delta_3 \\
H_{SO}{}^3\Delta_2 &= \frac{a_\delta}{\sqrt{2}}(\bar{\sigma}\delta - \sigma\bar{\delta}) + \frac{a_\delta}{\sqrt{2}}\sigma\pi &&= a_\delta {}^1\Delta_2 + \frac{a_\delta}{\sqrt{2}}{}^3\Pi_2 \\
H_{SO}{}^3\Delta_1 &= -a_\delta \bar{\sigma}\bar{\delta} + a_\delta \bar{\sigma}\pi &&= -a_\delta {}^3\Delta_1 + a_\delta \bar{\sigma}\pi,
\end{aligned} \tag{7}
$$

where the ${}^3\Pi$ state arises from the $5s\sigma 4d\pi$ configuration and $\bar{\sigma}\pi$ appears in

$$
{}^{3,1}\Pi_1 = \frac{1}{\sqrt{2}}(\bar{\sigma}\pi \pm \sigma\bar{\pi}). \tag{8}
$$

The parameter a_δ is the monoelectronic spin–orbit coefficient associated with the $d\delta$ electron (*25*).

From this calculation, it is clear that $X^3\Delta$ can only be perturbed by ${}^1\Delta(5s\sigma 4d\delta)$ and/or ${}^3\Pi$ or ${}^1\Pi(5s\sigma 4d\pi)$. For example, the rovibronic energies of each spin component ($v = 0$) can be calculated as

$$
\begin{aligned}
T({}^3\Delta_3) &\cong T_0 + a_\delta \\
T({}^3\Delta_2) &\cong T_0 - \frac{a_\delta^2}{\Delta E({}^1\Delta_2)} - \frac{a_\delta^2}{2\Delta E({}^3\Pi_2)} \\
T({}^3\Delta_1) &\cong T_0 - a_\delta - \frac{a_\delta^2}{2\Delta E({}^3\Pi_1)} - \frac{a_\delta^2}{2\Delta E({}^1\Pi_1)},
\end{aligned} \tag{9}
$$

where ΔE is the energy distances of the perturbing states (positive if this state is above the perturbed $X^3\Delta$ state).

Because of the number of unknown quantities, one must assume that there is a unique perturbing state. In the three cases ($^1\Pi$, $^3\Pi$, or $^1\Delta$) the orders of magnitude of the solutions for a_δ are the same. The $^1\Pi$ state is eliminated because it is found below the ground $X^3\Delta$ state; the $^3\Pi$ state is also eliminated because it is found too close to the $X^3\Delta$ state ($\Delta E \cong 800$ cm^{-1}); such a situation is not consistent with our perturbation procedure and should imply strong localized perturbations in the upper vibrational levels of the $X^3\Delta$ state, which have not been observed. One must note that similar $^1\Pi$ and $^3\Pi$ states are observed in ZrO at around 15 500 and 13 000 cm^{-1} (*6*, *27*) and in TiO at 14 800 and 12 000 cm^{-1} (*27*). The only satisfactory solution is a perturbation by a $^1\Delta(5s\sigma 4d\delta)$ state found around 4000 cm^{-1} above the $X^3\Delta_2$ substate[6]; the corresponding value of a_δ is 365.98 cm^{-1}. Similar calculations can be made with ZrO (resp. TiO) (*27*) where a $^1\Delta$ state is actually observed; one finds by this method $a_\delta = 312.75$ cm^{-1} and $\Delta E = 3938$ cm^{-1} instead of the observed 3260 cm^{-1} (resp. $a_\delta = 98.75$ cm^{-1} and 4150 cm^{-1} instead of 3340 cm^{-1}); this offers a check of our procedure. Note that with the hypothesis of a unique perturbing state, one need not be surprised by the fact that the calculated energy distances are higher than the observed ones, since the molecular states are never pure determinantals and the real interaction matrix elements always have a lower modulus than in the theoretically pure case.

2. *The Excited $A^3\Phi(\pi 4d\delta)$ State*

The representation of $A^3\Phi(\pi 4d\delta)$, where the π electron has probably a metallic $5p$ and $4d$ parentage, is

$$
\begin{aligned}
{}^3\Phi_4 &= \pi\delta \\
{}^3\Phi_3 &= \frac{1}{\sqrt{2}}(\bar{\pi}\delta + \pi\bar{\delta}) \\
{}^3\Phi_2 &= \bar{\pi}\bar{\delta}.
\end{aligned} \tag{10}
$$

The last member of this subset is the orthogonal $^1\Phi_3$ state:

$$
{}^1\Phi_3 = \frac{1}{\sqrt{2}}(\bar{\pi}\delta - \pi\bar{\delta}). \tag{11}
$$

The $^3\Pi$ and $^1\Pi$ states also arise from this configuration but we do not use them here. The possible perturbing states are $^1\Gamma_4(4d\delta^2)$, $^1\Phi_3(\pi 4d\delta)$, $^{1,3}\Delta(5p\pi 4d\pi)$, and $^{1,3}\Delta(\sigma 4d\pi)$ (these last ones with one $5p\sigma$ or one $4d\sigma$ electron). In all cases the values of a_π is between 700 and 762 cm^{-1}, that is, very close to $a_\delta/2$; this has as a peculiar consequence that the unique interaction of $A^3\Phi$ with the $^1\Phi_3(\pi 4d\delta)$ state is negligible because the corresponding interaction matrix element is proportional to $a_\delta - a_\pi/2$. Thus the $^1\Phi_3(\pi 4d\delta)$ state is eliminated: this is probably the most important reason for the low

[6] That is, absolutely, at around 4377 cm^{-1}.

value of the central shift δ_Φ in the $A^3\Phi$ state. We note that a similar situation arises in ZrO and TiO.

As in the $X^3\Delta$ case, with only one perturbing state, we find a $^1\Gamma_4$ perturbing state lying around 54 000 cm^{-1} (a_π = 732.42 cm^{-1}) or a $^3\Delta(\sigma 4d\delta)$ state far below the $A^3\Phi$ state, which is unsatisfactory (such a state is observed in ZrO around 23 550 cm^{-1} and in TiO around 19 500 cm^{-1} (*27*)). The better solutions are given by a $^3\Delta(5p\pi 4d\pi)$ state lying around 19 000 cm^{-1} (a_π = 761.98 cm^{-1}) and a $^1\Delta(5p\pi 4d\pi)$ or a $^1\Delta(\sigma 4d\delta)$ state lying between 19 000 and 29 000 cm^{-1} (a_π = 702.86 cm^{-1}).[7] Singlet Δ states are observed in ZrO around 24 520 cm^{-1} and in TiO around 22 570 cm^{-1} (*27*). As noted above, the real energy differences, and thus the positions given here, are probably lower than the calculated ones.

In the case of TiO, the central shift parameter δ_Φ (+2.35 cm^{-1}) is very small and the interpretation is not simple: it is probably produced by the effects of several weakly perturbing states. In the case of ZrO, δ_Φ is negative and its magnitude is about twice that of NbN. Among all the possibilities, one can note the prediction of a $^3\Delta(\sigma 4d\delta)$ perturbing state at an energy distance of 4800 cm^{-1} above the $^3\Phi(\pi 4d\delta)$ state (i.e., around 22 560 cm^{-1}); we noted above that such a $^3\Delta$ state lies around 23 550 cm^{-1}, 5800 cm^{-1} above the $^3\Phi$ state (*27*). This is probably not the only possibility because, as one can see, the calculated energy difference is less than the observed one in this case; but this is one possible origin for the reversed central shift δ_Φ of ZrO.

3. Line Broadening in the $A^3\Phi_2$–$X^3\Delta_1$ (0,0) Subband

One possible interpretation of this effect is a Λ doubling in the $X^3\Delta_1$ substate. This (fourth-order) phenomenon arises when the $^3\Delta_1$ spin component is perturbed by a $^{1,3}\Pi$ state and a $^{1,3}\Sigma_0$ substate sufficiently close to the $^3\Delta$ state. It is well known that a $^1\Sigma^+(5s\sigma^2)$ state lies at low energy near $X^3\Delta$ (*12*) and the presence of a perturbing singlet or triplet Π state can be assumed. Without any other experimental information, this explanation is at least a possible one.

One must note that a closer examination of this problem shows that this hypothesis can hardly be reconciled with the assumed electron configuration of $X^3\Delta(5s\sigma 4d\delta)$; this configuration leads to a $^{1,3}\Pi(5s\sigma 4d\pi)$ intermediate perturbing state and, above all, to $^{1,3}\Sigma^+(5s\sigma 4d\sigma)$ perturbing states instead of the $^1\Sigma^+(5s\sigma^2)$ one. No observation of such states at reasonable low energies has been made in YF, ZrO, or TiO. Such a consideration invites caution as to this origin of the broadening.

The explanation of a hyperfine spin-uncoupling effect (*20*) may, alternatively, be proposed. Figure 3, indeed, shows that the widened rotational lines may have a multiplet structure instead of the expected doublet structure in the case of a Λ doubling.

ACKNOWLEDGMENTS

We acknowledge the support of the National Science Foundation of Grant GP-38782 to one of us (T.M.D.) and the hospitality of the Chemistry Department of the University of Michigan at Ann Arbor (J.-L.F., C.A., and K.M.R.).

RECEIVED: March 5, 1987

[7] In the case of a perturbation by a $^1\Delta_2$ state, only the $^3\Delta_2$ substate is shifted toward the lower energies: this explains the low value of a_π.

REFERENCES

1. U. UHLER, *Ark. Fys.* **8,** 265–279 (1954).
2. T. M. DUNN, *in* "Molecular Spectroscopy: Modern Research" (K. Narahari Rao and C. W. Mathews, Eds.), Academic Press, New York, 1972.
3. L. AKERLIND, *Naturwissenschaften* **9,** 375–376 (1961); *Ark. Fys.* **22,** 41–64 (1962).
4. C. K. JORGENSEN, *Mol. Phys.* **1,** 417–424 (1964).
5. T. M. DUNN, XIII Colloq. Spectrosc. Intern., Ottawa, 1967.
6. L. J. LAUCHLAN, J. M. BROM, JR., AND H. P. BROIDA, *J. Chem. Phys.* **65,** 2672–2678 (1976).
7. R. STRINGAT, C. ATHENOUR, AND J.-L. FEMENIAS, *Canad. J. Phys.* **50,** 395–403 (1972).
8. A. ADAMS, W. KLEMPERER, AND T. M. DUNN, *Canad. J. Phys.* **46,** 2213–2220 (1968).
9. C. W. BAUSCHLICHER, JR., AND S. R. LANGHOFF, *J. Chem. Phys.* **85,** 5936–5942 (1986).
10. T. M. DUNN AND K. M. RAO, *Nature (London)* **222,** 266–267 (1969).
11. D. W. GREEN, W. KORFMACHER, AND D. M. GRUEN, *J. Chem. Phys.* **58,** 404–405 (1975).
12. N. L. RANIERI, PH.D. thesis, Department of Chemistry, University of Michigan (1979).
13. C. ATHENOUR, J.-L. FEMENIAS, AND T. M. DUNN, International Colloquium on High Resolution Molecular Spectroscopy, Tours, France, 1975.
14. C. ATHENOUR, Thesis, C.N.R.S. A.O.11.500 Nice, France (1975).
15. J.-L. FEMENIAS, C. ATHENOUR, AND T. M. DUNN, *J. Chem. Phys.* **63,** 2861–2868 (1975).
16. T. L. PORTER AND S. P. DAVIS, *J. Opt. Soc. Amer.* **53,** 338–343 (1963); D. M. EAKIN AND S. P. DAVIS, *J. Mol. Spectrosc.* **35,** 27–42 (1970).
17. H. E. RADFORD, *Phys. Rev. A* **136,** 1571–1575 (1964); K. M. EVENSON, J. L. DUNN, AND H. P. BROIDA, *Phys. Rev. A* **136,** 1566–1571 (1964); R. L. BARGER, H. P. BROIDA, A. J. ESTIN, AND H. E. RADFORD, *Phys. Rev. Lett.* **9,** 345–346 (1962).
18. R. F. BARROW, W. J. M. GISSANE, AND R. RICHARDS, *Proc. R. Soc. A* **300,** 469–486 (1967); W. ATKINS, *Proc. R. Soc. A* **300,** 487–495 (1967).
19. E. A. PAZYUK, E. N. MOSKVITINA, AND YU. YA. KUZYAKOV, *Spectrosc. Lett.* **19,** 627–638 (1986).
20. J.-L. FEMENIAS, G. CHEVAL, A. J. MERER, AND U. SASSENBERG, *J. Mol. Spectrosc.* **124,** 348–368 (1987).
21. R. C. CARLSON, J. K. BATES, AND T. M. DUNN, *J. Mol. Spectrosc.* **110,** 215–241 (1985).
22. R. N. ZARE, A. L. SCHMELTEKOPF, W. J. HARROP, AND D. L. ALBRITTON, *J. Mol. Spectrosc.* **46,** 37–66 (1973).
23. I. KOVACS, "Rotational Structure in the Spectra of Diatomic Molecules," Adam Hilger Ltd., London, 1969.
24. L. VESETH, *Mol. Phys.* **26,** 101–107 (1973).
25. H. LEFEBVRE-BRION AND R. W. FIELD, "Perturbations in the Spectra of Diatomic Molecules," Academic Press, New York, 1986.
26. C. FROESE FISCHER, *At. Data* **4,** 301–399 (1972).
27. K. P. HUBER AND G. HERZBERG, "Constants of Diatomic Molecules," Van Nostrand-Reinhold, New York, 1979.
28. R. S. MULLIKEN, *Rev. Mod. Phys.* **3,** 89–155 (1931).
29. E. A. SHENYAVSKAYA AND L. V. GURVICH, *J. Mol. Spectrosc.* **68,** 41–47 (1977).
30. D. L. ALBRITTON, A. L. SCHMELTEKOPF, AND R. N. ZARE, *in* "Molecular Spectroscopy: Modern Research" (K. Narahari Rao, Ed.), Vol. 2, pp. 1–67, Academic Press, New York, 1976.
31. J.-L. FEMENIAS, Communication at the Xth Colloquium on High Resolution Molecular Spectroscopy, Dijon, France, 1987.
32. A. J. MERER, *Mol. Phys.* **23,** 309–315 (1972).
33. R. M. CLEMENTS AND R. F. BARROW, *Trans. Faraday Soc.* **65,** 1163–1167 (1969).